Desalination and Water Treatment
www.deswater.com

doi: 10.5004/dwt.2020.24957

178 (2020) 240–253
February

Combined influence of some cations on arsenic removal by an air-injection EC reactor using aluminum ball electrodes

A.Y. Gören[a,*], M. Kobya[b], E. Şık[c], E. Demirbas[d], M.S. Oncel[b]

[a]Department of Environmental Engineering, İzmir Institute of Technology, 35430 İzmir, Turkey, Tel. +90 232 750 6670; email: yagmurgoren@iyte.edu.tr
[b]Department of Environmental Engineering, Gebze Technical University, 41400 Gebze, Turkey, Tel. +90 262 6053214; emails: kobya@gtu.edu.tr (M. Kobya), soncel@gtu.edu.tr (M.S. Oncel)
[c]Environment and Cleaner Production Institute, Tübitak Marmara Research Center, 41470 Gebze, Turkey, Tel. +90 262 6053160; email: cvemrah@gmail.com
[d]Department of Chemistry, Gebze Technical University, 41400 Gebze, Turkey, Tel. +90 262 6053010; email: erhan@gtu.edu.tr

Received 21 February 2019; Accepted 22 September 2019

ABSTRACT

Combined effects of some cations such as calcium (Ca^{2+}), iron (Fe^{2+}), manganese (Mn^{2+}), and magnesium (Mg^{2+}) and operating time on the removal of arsenic by air-injected electrocoagulation (EC) reactor with aluminum (Al) ball electrodes were investigated. The operating conditions were optimized with the Box–Behnken design of response surface methodology (RSM). The response variables were selected from the program as removal efficiency, residual arsenic concentration, energy consumption and operating cost (OC) in the EC process. A total of 46 experimental run was performed. The removal efficiency of arsenic increased with an increase in iron concentration (0.5–4.5 mg/L). The rest of the cations showed no noticeable effect on arsenic removal efficiency. The maximum arsenic removal efficiency and minimum OC at the optimum operating conditions (C_{Ca}: 305 mg/L, C_{Mg}: 42 mg/L, C_{Fe}: 3.3 mg/L, C_{Mn}: 2.34 mg/L, initial pH of 7.5 applied current of 0.15 A, Al ball size of 7.5 mm, 5.0 cm of Al ball anodes height in the EC reactor, air-fed rate of 6.0 L/min and t_{EC}: 16.83 min) in the EC process were 99.9% and 0.0332 $/m^3 for initial arsenic concentration of 200 μg/L, respectively. The removal mechanism of As(III) by EC seems to be oxidation of As(III) to As(V) and subsequent removal by adsorption/complexation with aluminum hydroxides generated in the process. The results showed that the air-injected EC reactor can be used effectively for arsenic and hardness removal simultaneously from real groundwater sources.

Keywords: Arsenic removal; Cation effect; Electrocoagulation; Al electrode; Optimization

1. Introduction

Globally, groundwater is a critical source of drinking water supply. However, arsenic contamination in groundwater sources has been well documented in the literature which shows a very large range from 0.5 to 5,000 ppb covering more than 70 countries [1]. Groundwater arsenic contaminations are observed in vast regions including Gangetic delta in Bangladesh, West Bengal delta basin in India, Pamplonian and Chaco-Pampean plains in Argentina, Antofagasta in Northern Chile, Mekong and Red River basins in Vietnam and Cambodia, Hetao Basin in Inner Mongolia in China and southwest Taiwan in the world [2,3]. People in Turkey are also threatened by arsenic contamination, and several

---

[*] Corresponding author.

1944-3994/1944-3986

cases of arsenic pollution in geothermal and groundwater in mining basins such as borate deposit, mercury, gold, lead-zinc in West Anatolia have also been observed with concentrations of arsenic ranging from 1 to 10,700 μg/L [4]. Arsenic contamination of natural waters arises from the dissolution and weathering of arsenic-containing minerals as well as various human activities [5].

Exposure to drinking water containing arsenic leads to various acute and chronic health problems including skin lesions like hyperkeratosis liver and cardiovascular problems, gastro-intestinal, respiratory diseases, and cancer [6]. Therefore, the United States Environmental Protection Agency (US-EPA) and the World Health Organization (WHO) have decreased the maximum recommended arsenic contaminant level from 50 to 10 μg/L for drinking water [7,8]. Therefore, arsenic removal from groundwater has become an issue that attracts great interest in diverse groups. To achieve recommended arsenic contaminant level in drinking waters, the US-EPA has offered some of the best available removal processes such as modified electro-dialysis (85%), coagulation-filtration (95%), lime softening (90%), activated alumina (95%), and ion-exchange (95%) [9]. Additionally, the US-EPA has suggested emerging arsenic treatment processes, namely, manganese greensand filtration, adsorption using zero-valent iron, iron filings, and granular ferric hydroxide [5]. Recently, the different functionalized nanomaterials were also used for harmful organic compounds (As, Cr(II), Pb(II), Cs, Cu (II), Hg (II), Pd(II)) removal from aqueous solutions [10–15]. For instance, Awual [16] used a novel facial composite adsorbent for copper(II) removal from wastewater. Awual [16] reported that the highest copper sorption capacity was obtained at 10 mg adsorbent dosage and the copper adsorption capacity of novel adsorbent was 176.27 mg/g. In a separate study, removal of Pd(II) from synthetic water was investigated using ligand-based conjugate nanomaterials. They observed that the highest Pd(II) adsorption capacity was 157.23 mg/g for optimum adsorbent amount of 10 mg [17]. The mesoporous adsorbent was also used for Pd(II) and Cu(II) removal from aqueous solution. They observed that the maximum adsorption capacity was 172.53 mg/g for Pd(II) and 182.39 mg/g for Cu(II) [18].

Among the treatment methods recommended by US-EPA, the coagulation/filtration technology is simple; only common chemicals are used, installation costs are small and can be easily applied to large water volumes. However, this technology is not as efficient for As(III), and peroxidation of As(III) to As(V) using some oxidizing chemical agents like chlorine, potassium permanganate, and hypochlorite is necessary for better removal efficiency. The lime softening is efficient to treat water containing arsenic with high hardness at pH > 10.5, but it is required for pre-oxidizing of As(III), pH adjustment and high coagulant dose. The adsorption results in a low rate of removal efficiency for As(III). The ion exchange is also effective for the removal of As(V) except for the operating cost (OC) due to resin type and resin regeneration. Currently, the available membranes such as microfiltration, nanofiltration, and reverse osmosis are more expensive than the other arsenic removal options because of high electrical consumption, relatively high capital and OC and the risk of membrane fouling. These drawbacks of the available options have forced the researchers to find novel alternative treatment processes or to enhance commonly used treatment processes with modifications. The electrocoagulation (EC) process has attracted attention for the treatment of arsenic from groundwater as a result of such benefits its capability to remove trace levels of arsenic, operational simplicity, treatment compactness, cost-effectiveness removal to low arsenic concentrations, reduced amount of sludge formation and no need for additional chemical reagents [19,20]. Recently, EC has been employed for the removal of arsenic from groundwater in the literature [21,22]. These studies mainly focused only on arsenic content in the groundwater. However, those waters do not represent the same chemical composition of actual groundwater. In real groundwater, a large amount of coexisting anions and cations are present depending on the environment in which the groundwater source is located. These ions are known to interact with metal hydroxide surfaces and may compete with arsenic for adsorption. Anions and cations might influence the adsorption of arsenic negatively or positively [23]. It is well known in arsenic removal by chemical coagulation that some anions (i.e., phosphate, molybdate, silicate, fluoride, bicarbonate) compete with arsenic for metal oxides surfaces and affect adsorption of arsenic with electrostatic charge at the metal oxides surface like $Al(OH)_3$ and $Fe(OH)_3$ [24]. Also, competition between arsenate/arsenite and cations (i.e., iron, manganese) may affect the performance of arsenic removal by the EC treatment process in groundwater.

In the aqueous environment, inorganic arsenic appears commonly in forms of arsenite (As(III)) and arsenate (As(V)). pH, redox potential and the presence of complexing ions such as ions of sulfur, aluminum, and calcium determine the arsenic valence and speciation. The nature of the interaction of ions at interfaces has been a longstanding and difficult problem to fully unravel. The behavior of ions near the air-water interface and uncharged hydrophobic solid surfaces has been the subject of many experimental studies and simulations of ions at the air-water interface gave crucial insight into the order of the Hofmeister series [25–28]. Generally, anions show more specific and more pronounced effects than cations. This distinction can be explained by the fact that anions are commonly bigger and more polarizable than cations. The Hofmeister selectivity response toward arsenic over other anions might be proposed with a sequence order of $NO_3^- > Cl^- > SO_4^{2-}$.

However, there is still a need for further research concentrating on not enough investigations on the effect of cations on the arsenic removal. In addition, cations with multiple effects on the arsenic removal has not been investigated in the literature. Moreover, cations and anions in water affect the conductivity of the solution and cell voltage. Cations such as calcium, magnesium, sodium, and manganese increase water conductivity which leads to a decrease in power consumption and OC [29]. Thus, the cations concentrations and speciation effect should be considered for a thorough evaluating of arsenic removal from groundwater in the EC process. Generally, plate and rod types of sacrificial electrodes are used in the EC reactors. These electrodes have some disadvantages in that they are not efficient in terms of changing and maintenance, and they have limited surface areas. Consequently, an air-injected EC reactor with Al and Fe ball electrodes has been developed recently to deal with these problems [21,30,31]. The new designed EC reactor with Al ball electrodes has features of process compactness, simplicity to use, higher electrode surface areas and significant removal efficiency.

Compared to the EC studies in the literature, this paper is the first to investigate the multiple effects of cations present in groundwater containing arsenic using the new EC reactor with Al ball electrodes. Employing this method can handle the groundwater by treating arsenic and other cations (Ca^{2+}, Fe^{2+}, Mg^{2+}, and Mn^{2+}) simultaneously. It can also reduce the effluent arsenic concentration below the recommended level, prevent the passivation layer on the electrode surface by airflow, and reduce the sludge formation in the new EC reactor. In this study, cations' (Ca^{2+}, Fe^{2+}, Mg^{2+}, and Mn^{2+}) effects on the arsenic removal was evaluated with the newly designed EC reactor using Al ball electrodes. The effects of cations' concentrations and operating time on removal were analyzed. A 3-level Box–Behnken design (BBD) with responses (removal efficiency (R_e (%)), OC (\$/m^3), arsenic adsorption capacity (q_e (μg As/g Al)), energy (energy consumption (ENC) (kWh/m^3)) and electrode consumptions (ELC (kg/m^3)) were studied.

2. Arsenic removal mechanism in the EC process

The EC process consists of electrochemical dissolution of an anode like Al and concurrent H_2 formation from the cathode surface. In the case of Al anode in the EC process, this resulted with the electrodissolution of the Al at the anode (Eq. (1)) and the reduction of water at the cathode (Eq. (2)) producing aluminum and hydroxide ions as shown in the following reactions [29,32]:

$$\mathrm{Al}_{(s)} \rightarrow \mathrm{Al}^{3+} + 3\mathrm{e}^- \tag{1}$$

$$3\mathrm{H_2O} + 3\mathrm{e}^- \rightarrow {}^{3}\!/_{2}\,\mathrm{H_2} + 3\mathrm{OH}^- \tag{2}$$

The type of aluminum hydroxides ($Al_x(OH)_y$) produced during the EC is quite variable and is predominantly affected by pH. As a result, polymerization reactions in the solution can convert into various monomeric and polymeric Al hydroxide species as Eq. (3) [33]:

$$x\mathrm{Al}^{3+} + y\mathrm{OH}^- \rightarrow \text{Monomoricand polymeric } \mathrm{Al}_x\left(\mathrm{OH}\right)_y^{3x-y} \text{ Species} \rightarrow \mathrm{Al}\left(\mathrm{OH}\right)_{3(s)} \tag{3}$$

The trivalent aluminum (Al^{3+}) and hydroxide ions (OH^-) generated at the anode and cathode electrodes, respectively, and react to form monomeric species like $Al(OH_4^-)$, $Al(OH)_2^+$, $Al(OH)^{2+}$, and $Al_2(OH)_2^{4+}$, and polymeric species like $Al_6(OH)_{15}^{3+}$, $Al_7(OH)_{17}^{4+}$, $Al_8(OH)_{20}^{4+}$, $Al_{13}(OH)_{34}^{5+}$, and $Al_{13}O_4(OH)_{21}^{7+}$ at pH 3–11 [30,32]. At pH 4.0–9, these monomeric and polymeric species are transformed into $Al(OH)_{3(s)}$. At pH values greater than 9.5, the $Al(OH_4^-)$ complex formation also occurs in the solution according to Eq. (4). These $Al(OH_4^-)$ ions are soluble and do not have any influence on the contaminant removal from solution [34].

$$2\mathrm{Al} + 6\mathrm{H_2O} + 2\mathrm{OH}^- \rightarrow 2\mathrm{Al}\left(\mathrm{OH}_4^-\right) + 3\mathrm{H_2} \tag{4}$$

The major arsenic species in solution in the pH range of 2.7–11.5 is $H_2AsO_4^-$ and $HAsO_4^{2-}$. The arsenic removal is believed to adsorb arsenic species onto produced aluminum hydroxides flocs and surface complexation reactions (Eqs. (5)–(7)):

$$\equiv \mathrm{Al-OH} + \mathrm{H_2AsO_4^-} \rightarrow \equiv \mathrm{Al-H_2AsO_4} + \mathrm{OH}^- \tag{5}$$

$$\equiv \mathrm{Al-OH} + \mathrm{HAsO_4^{2-}} \rightarrow \equiv \mathrm{Al-HAsO_4} + \mathrm{OH}^- \tag{6}$$

$$\mathrm{Al}\left(\mathrm{OH}\right)_{3(s)} + \mathrm{AsO}_{4(aq)}^{3-} \rightarrow \left[\mathrm{Al}\left(\mathrm{OH}\right)_3 \times \mathrm{AsO_4^{3-}}\right]_{(s)} \tag{7}$$

The isoelectric point (pH_{pzc}) of $Al(OH)_3$ and Al_2O_3 is found at pH 8.3 and 8.4–9.1, respectively [35]. The surfaces of aluminum hydroxide and aluminum oxide at pH lower than 8 are predominantly positively charged. Maximum adsorption of arsenate (98.6%) and arsenite (96%) were obtained with high affinity towards alumina surfaces at pH 5.8 and 7.6 [36]. Therefore, it is concluded that arsenic species in solution are adsorbed on the surfaces of $Al(OH)_3$ and Al_2O_3 during the adsorption process [37].

3. Materials and methods

3.1. Characteristics of groundwater and analytical procedure

The real groundwater sample was taken from Kocaeli province in Turkey The groundwater containing 200 μg/L of total arsenic (100 μg/L As(III) + 100 μg/L As(V)) was daily prepared by dissolving sodium arsenate for As(V) and sodium arsenite salts. The groundwater sample has the following compositions: calcium (152 mg/L), chloride (127 mg/L), magnesium (15 mg/L), nitrate (2 mg/L), sodium (22 mg/L), sulphate (94.2 mg/L), total Si (10 mg/L), $CaCO_3$ (260 mg/L), total dissolved solids (TDS) (528 mg/L), total organic carbon (TOC) (5 mg/L), a pH of 7.5, and electrical conductivity of 1.30 mS/cm. Iron, manganese, phosphorus, and arsenic were not detected in the sample. Then, the groundwater samples were prepared by dissolving the pre-weighed amount of magnesium, calcium, iron and manganese inorganic salts based on the experimental design. The groundwater quality was determined according to standard methods [38]. The arsenic concentration in the groundwater was determined using an inductively coupled plasma optical emission spectrometry (ICP-OES, PerkinElmer Optima 7000 DV, USA) before and after the experiments. The concentrations of cations (Ca^{2+}, Mg^{2+}, Fe^{2+}, and Mn^{2+}) and anions (NO_3^-, SO_4^{2-}, PO_4^-, and Cl^-) were measured by ICP-OES and by ion chromatography (IC, Shimadzu HIC-20A, USA), respectively. TOC was determined by the TOC analyzer (Shimadzu, TOC-L model). The measurements of pH, conductivity, and TDS were achieved with a pH meter (Mettler Toledo Seven Compact, USA) and conductivity meter (Mettler Toledo, USA), respectively. All experiments in this study were performed twice and the average results were taken.

3.2. Air-injected EC reactor and experimental procedure

Fig. 1 shows a schematic diagram of the air-injected batch EC reactor (volume of 2,041 cm^3; diameter of 100 mm and height of 260 mm). The construction of the new EC reactor was reported in previous works [19,21]. Al balls as anode material and titanium (Ti) as cathode material (255 mm × 70 mm × 3 mm) were used in the new EC reactor. 800 mL of groundwater containing 200 µg/L of total arsenic and specified amount of cations fed into the new EC reactor. The operating parameters (applied current of 0.15 A, Al ball size of 7.5 mm, anode height of 5 cm in the EC reactor, initial pH of 7.5 and airflow rate of 6 L/min) were adjusted according to the earlier studies [30]. Then, the connection between the anode and cathode was maintained by the direct current (DC) power supply (Agilent 6675A, USA). Before starting, the electrical current of the system was set to a pre-established value using the DC power supply. An air-injection diffuser was attached under the reactor and the air was supplied continuously to the EC reactor for sedimentation of generated sludge as $Al(OH)_{3(s)}$ flocs between Al ball anodes and to maintain uniform stirring in the reactor.

3.3. Box–Behnken experimental design and statistical analysis

Response surface methodology (RSM) is a combination of statistical and mathematical techniques used for optimizing and improving processes. RSM is an effective technique for the optimization of the process when the combination of various independent operational variables and interactions between these variables affect desired results [39]. Therefore, the BBD is the most common RSMs, which is used for the optimization of the arsenic removal to obtain maximum R_e, minimum OC, and determine the impact of independent operational variables on the arsenic removal. Design Expert 8.0.4.1 was used for the statistical design of experiments and data analysis. The BBD also reduced the required number of experimental runs with high interactive effects between the independent operational parameters.

In this model, calcium (x_1), magnesium (x_2), iron (x_3), manganese (x_4) concentrations and operating time (x_5) were considered as the independent variables. As shown in Table 1, the low, middle and high concentrations of each independent operational variable were designated as (–1), (0) and (+1), respectively. Other operating parameters such as current density, Al ball size, the height of anode electrode in the EC reactor, pH and airflow rate were kept constant. According to the BBD matrix produced by the Design Expert program, a total of 46 experimental runs was performed (Table 2). The experimental runs were randomized to minimize (OC) or maximize (R_e). The effects of unexplained variability in the observed responses such as R_e, ELC, ENC, OC, and q_e are presented in Tables 2 and 3.

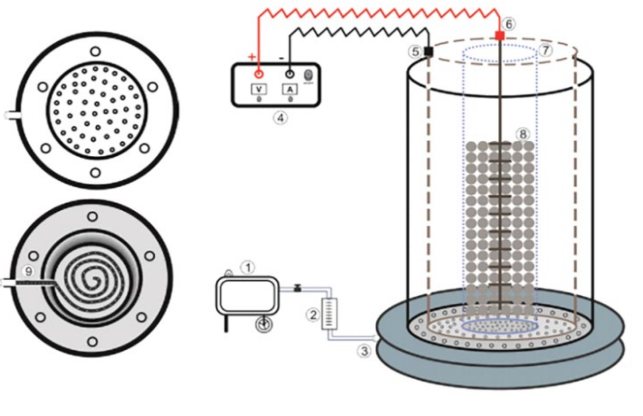

Fig. 1. Air-injection EC reactor (1: air compressor, 2: flow meter, 3: air diffuser line, 4: power supply, 5: Ti cathode, 6: steel rod contact with Al ball electrodes, 7: inner cylindrical-shaped Plexiglas put into Al ball anodes, 8: Al ball anodes, and 9: air diffuser).

OC of the EC process includes electrodes and electrical energy costs, but do not include maintenance of the reactor, labor, sludge disposal, and fixed costs. The latter costs of components were mostly uncontrolled by the type of electrode materials. Therefore, OC of the arsenic removal in the EC process was calculated based on two parameters: the amount of energy and consumption of the electrode material (Eq. (8)).

$$\text{OC}\left(\$/\text{m}^3\right) = \alpha\text{ENC} + \beta\text{ELC} \tag{8}$$

where α is the unit electrical energy price (0.19 \$/kWh) and β is the unit Al electrode price (15 \$/kg) according to the Turkish Market in October 2018. The ENC and ELC for the arsenic removal were calculated by the following equations:

$$\text{ENC}\left(\text{kWh}/\text{m}^3\right) = \frac{U \times i \times t_{\text{EC}}}{v} \tag{9}$$

$$\text{ELC}\left(\text{kg}/\text{m}^3\right) = \frac{i \times t_{\text{EC}} \times M_{\text{Al}}}{z \times F \times v} \tag{10}$$

where U is the voltage (V), i is the applied current (A), t_{EC} is the EC time (min) and v is volume of the groundwater in the new EC reactor (m^3), M_{Al} is the molecular weight of the Al (26.98 g/mol), z is the number of electrons (z:3), and F is the Faraday's constant (96487 C/mol).

Charge loading (q, Coulomb) is explained as the charges transferred in electrochemical reactions for a given amount of water removed in the EC reactor and is defined by:

$$q(C) = i \times t_{\text{EC}} \tag{11}$$

Table 1
Independent operational variables and concentrations for three-level factorial study of the arsenic removal

Independent variables	Levels of independent variables		
	(–1)	(0)	(+1)
x_1:C_{Ca} (mg/L)	125	225	325
x_2:C_{Mg} (mg/L)	15	35	55
x_3:C_{Fe} (mg/L)	0.5	2.5	4.5
x_4:C_{Mn} (mg/L)	0.5	2.5	4.5
x_5:t_{EC} (min)	8	15	22

Table 2
Experimental plan for investigation of cations effect on As removal using a BBD

Exp. run	x_1:Ca (mg/L)		x_2:Mg (mg/L)		x_3:Fe (mg/L)		x_4:Mn (mg/L)		x_5:t_{EC} (min)	$C_{f,As}$	$R_{e,As}$
	$C_{0,Ca}$	$C_{f,Ca}$	$C_{0,Mg}$	$C_{f,Mg}$	$C_{0,Fe}$	$C_{f,Fe}$	$C_{0,Mn}$	$C_{f,Mn}$	(t_{EC})	(µg/L)	(%)
1	225	206.2	35	29.9	0.5	0.40	2.5	1.10	22	1.78	99.11
2	225	212.6	15	14.3	4.5	0.71	2.5	1.25	15	0.63	99.69
3	325	314.3	35	31.8	2.5	0.96	2.5	0.91	8	29.40	85.30
4	225	215.8	35	32.6	2.5	0.70	4.5	1.68	8	34.35	82.83
5	125	122.5	35	34.1	2.5	0.97	2.5	0.85	8	36.75	81.63
6	325	320.8	35	33.2	2.5	1.36	4.5	1.35	15	3.21	98.40
7	325	312.0	35	31.4	0.5	1.46	2.5	0.65	15	8.46	95.77
8	225	208.6	35	32.6	4.5	1.09	2.5	0.54	8	18.80	90.60
9	225	222.6	35	33.9	0.5	0.14	0.5	0.21	15	16.50	91.75
10	225	211.7	15	15.6	2.5	1.23	4.5	1.53	15	5.68	97.16
11	225	201.7	35	31.6	2.5	1.01	2.5	0.95	15	4.27	97.87
12	225	208.8	35	31.1	2.5	0.70	2.5	0.85	15	4.98	97.51
13	225	220.1	55	50.7	2.5	0.89	0.5	0.15	15	0.12	99.94
14	325	317.3	35	32.0	2.5	1.68	2.5	1.12	22	0.19	99.91
15	125	114.8	35	31.7	2.5	0.44	0.5	0.18	15	6.84	96.58
16	225	208.0	15	13.1	2.5	1.71	0.5	0.11	15	5.26	97.37
17	125	117.0	35	30.8	2.5	1.03	4.5	1.25	15	5.96	97.02
18	225	238.9	55	53.1	2.5	1.48	2.5	0.84	8	33.70	83.15
19	225	215.2	35	33.2	2.5	0.64	0.5	0.07	22	1.56	99.22
20	325	321.1	55	50.4	2.5	1.87	2.5	0.45	15	3.93	98.04
21	325	320.5	15	14.8	2.5	2.10	2.5	0.78	15	4.03	97.99
22	325	321.4	35	34.2	2.5	2.09	0.5	0.06	15	5.10	97.45
23	225	202.0	35	34.5	2.5	1.34	2.5	0.66	15	0.45	99.78
24	225	223.2	15	14.7	0.5	0.19	2.5	0.98	15	9.32	95.34
25	325	320.0	35	32.7	4.5	1.65	2.5	0.75	15	1.12	99.44
26	225	241.2	55	52.5	4.5	0.61	2.5	0.70	15	3.31	98.35
27	225	208.4	15	10.7	2.5	0.44	2.5	0.64	22	1.05	99.48
28	225	209.4	35	14.6	2.5	0.94	4.5	1.63	22	0.94	99.53
29	225	209.8	55	54.3	2.5	1.16	2.5	1.32	22	0.90	99.55
30	225	207.7	35	32.9	2.5	0.64	2.5	1.21	15	6.58	96.71
31	225	196.1	35	29.9	4.5	0.70	2.5	1.21	22	0.05	99.98
32	125	107.8	35	30.5	0.5	0.25	2.5	0.93	15	17.95	91.03
33	225	201.8	55	51.6	2.5	0.90	4.5	1.32	15	3.15	98.43
34	225	220.5	35	34.8	2.5	0.27	0.5	0.13	8	29.90	85.05
35	225	221.8	55	56.9	0.5	0.58	2.5	0.87	15	9.07	95.47
36	225	214.5	35	32.9	4.5	0.60	4.5	1.65	15	0.70	99.65
37	225	208.5	35	30.6	4.5	2.07	0.5	0.09	15	0.98	99.51
38	125	105.4	15	12.5	2.5	0.56	2.5	0.93	15	5.05	97.48
39	225	190.5	35	29.0	0.5	0.36	4.5	1.92	15	10.52	94.74
40	125	116.6	55	52.0	2.5	0.08	2.5	1.12	15	4.22	97.89
41	125	112.5	35	27.8	4.5	0.19	2.5	1.23	15	0.79	99.61
42	125	102.8	35	27.2	2.5	0.49	2.5	0.84	22	0.70	99.55
43	225	209.6	35	32.3	0.5	0.43	2.5	0.56	8	39.25	80.38
44	225	191.7	35	30.6	2.5	0.28	2.5	0.78	15	5.50	97.25
45	225	197.3	35	26.7	2.5	0.40	2.5	0.63	15	3.07	98.47
46	225	204.1	15	14.4	2.5	0.49	2.5	0.84	8	33.48	83.26

Table 3
Experimental results for removal of arsenic from the groundwater in the EC process

Exp. run	pH_f	U	q	ENC	M_{Al}	ELC	OC	W_{sludge}	q_e	
	(–)	(V)	(C)	(kWh/m^3)	(mg)	(kg/m^3)	(\$/m^3)	(kg/m^3)	(μg As/mg Al)	(μg As/C)
1	7.68	12.37	198	0.8504	18.45	0.0081	0.205	0.02309	8.59	0.80
2	7.73	12.21	135	0.5723	12.58	0.0045	0.133	0.01574	12.67	1.18
3	7.87	8.85	72	0.2213	6.71	0.0025	0.055	0.00839	20.32	1.90
4	7.57	11.60	72	0.2900	6.71	0.0018	0.065	0.00839	19.73	1.84
5	7.59	16.16	72	0.4040	6.71	0.0066	0.112	0.00839	19.45	1.81
6	7.53	9.28	135	0.4350	12.58	0.0076	0.123	0.01574	12.50	1.17
7	6.63	9.26	135	0.4341	12.58	0.0084	0.127	0.01574	12.17	1.14
8	6.96	12.07	72	0.3018	6.71	0.0058	0.088	0.00839	21.58	2.01
9	7.75	11.62	135	0.5447	12.58	0.0065	0.138	0.01574	11.66	1.09
10	6.91	12.04	135	0.5644	12.58	0.0110	0.166	0.01574	12.35	1.15
11	6.51	11.85	135	0.5555	12.58	0.0128	0.173	0.01574	12.43	1.16
12	7.10	11.91	135	0.5583	12.58	0.0029	0.121	0.01574	12.39	1.16
13	7.31	10.61	135	0.4973	12.58	0.0026	0.108	0.01574	12.70	1.18
14	6.76	9.41	198	0.6469	1845	0.0013	0.130	0.02309	8.66	0.81
15	7.34	16.11	135	0.7552	12.58	0.0044	0.167	0.01574	12.27	1.14
16	7.45	12.29	135	0.5761	12.58	0.0039	0.130	0.01574	12.37	1.15
17	7.16	15.37	135	0.7205	12.58	0.0081	0.180	0.01574	12.33	1.15
18	7.56	10.24	72	0.2560	6.71	0.0061	0.081	0.00839	19.81	1.85
19	6.90	12.11	198	0.8326	18.45	0.0083	0.202	0.02309	8.60	0.80
20	7.34	8.75	135	0.4102	12.58	0.0015	0.086	0.01574	12.46	1.16
21	6.90	9.85	135	0.4617	12.58	0.0031	0.104	0.01574	12.45	1.16
22	7.20	9.32	135	0.4369	12.58	0.0076	0.123	0.01574	12.38	1.15
23	7.10	10.00	135	0.4688	12.58	0.0100	0.142	0.01574	12.68	1.18
24	7.31	12.04	135	0.5644	12.58	0.6051	0.314	0.01574	12.11	1.13
25	7.69	8.75	135	0.4102	12.58	0.0043	0.101	0.01574	12.63	1.18
26	7.07	11.16	135	0.5231	12.58	0.0116	0.161	0.01574	12.50	1.17
27	7.28	12.09	198	0.8312	18.45	0.0133	0.228	0.02309	8.62	0.80
28	6.74	12.09	198	0.8312	18.45	0.0078	0.199	0.02309	8.62	0.80
29	6.81	11.19	198	0.7693	18.45	0.0046	0.171	0.02309	8.62	0.80
30	6.84	11.90	135	0.5578	12.58	0.0081	0.149	0.01574	12.29	1.15
31	6.86	11.72	198	0.8058	18.45	0.0325	0.326	0.02309	8.66	0.81
32	7.32	17.28	135	0.8100	12.58	0.0336	0.332	0.01574	11.57	1.08
33	6.97	10.70	135	0.5016	12.58	0.0008	0.100	0.01574	12.51	1.17
34	7.25	11.66	72	0.0415	6.71	0.0133	0.078	0.00839	20.26	1.89
35	6.84	11.40	135	0.5344	12.58	0.0024	0.114	0.01574	12.13	1.13
36	6.90	11.30	135	0.5297	12.58	0.0011	0.106	0.01574	12.66	1.18
37	6.52	12.15	135	0.5695	12.58	0.0031	0.125	0.01574	12.64	1.18
38	6,89	18.29	135	0.8573	12.58	0.0029	0.178	0.01574	12.39	1.16
39	6.76	11.66	135	0.5466	12.58	0.0015	0.112	0.01574	12.04	1.12
40	7.23	14.28	135	0.6694	12.58	0.0056	0.157	0.01574	12.44	1.16
41	7.59	15.39	135	0.7214	12.58	0.0036	0.156	0.01574	12.66	1.18
42	7.48	16.91	198	1.1626	18.45	0.0096	0.272	0.02309	8.66	0.81
43	7.06	11.87	72	0.2968	6.71	0.4909	2.658	0.00839	19.15	1.79
44	7.20	12.15	135	0.5695	12.58	0.0003	0.110	0.01574	12.36	1.15
45	6.98	11.93	135	0.5592	12.58	0.0010	0.112	0.01574	12.51	117
46	7.04	12.23	72	0.3058	6.71	0.2258	1.255	0.00839	19.84	1.85

The arsenic adsorption capacity per amount of electrochemically dissolved electrode material was calculated from Eq (12):

$$q_e = \frac{\left(C_i - C_t\right) \times v}{\dfrac{\left(i \times t_{\mathrm{EC}} \times M_{\mathrm{Al}}\right)}{\left(z \times F\right)}} \qquad (12)$$

where C_i is initial arsenic concentrations (μg/L) and C_t is the arsenic concentrations at time *t* in the EC process.

4. Results and discussion

4.1. Effects of operational parameters on arsenic removal

The EC process is significantly intricate for the treatment of groundwater and can be affected by various operating parameters such as initial pH, applied current, airflow rate, operating time, size of anode material, anode height in the EC reactor, and ion concentrations. The optimum operational conditions, except different cations concentration and operating time, necessary for maximum arsenic removal efficiency were obtained from our previous papers [30]. At the present study, effects of cations' concentration and operating time were investigated to enhance the arsenic removal efficiency and to decrease the OC of the EC process Effects of independent variables (x_1:C_{Ca}, x_2: C_{Mg}, x_3:C_{Fe}, x_4:C_{Mn} and x_5:t_{EC}) on the arsenic removal efficiency were studied with responses from contour plots in Figs. 2a–d. These plots are helpful to understand both the main and the combined effects of operating time and cations.

Figs. 3a–f shows the interaction effects of two different cations on arsenic removal efficiency. Based on these graphics, the interacted effects of cations on the arsenic removal efficiency were discussed separately in the following sections.

4.2. Effects of calcium and magnesium on the arsenic removal

Among the hardness ions, calcium and magnesium are known as dominant species in groundwater containing anions such as arsenate and phosphate. In addition, high pH > 11 or high OH⁻ concentrations promote precipitation of the calcium and magnesium hardness in the form of $CaCO_3$ and $Mg(OH)_2$. On the other hand, pH is an important factor in the EC process which has a significant effect on forming metal hydroxide species, and removal mechanism of ions and contaminants. The pH increase in the EC process led to the formation of H_2 gas in the cathode electrode surface and accumulation of OH^- ions in the solution [32]. Ca^{2+} and Mg^{2+} may increase adsorption of As(V) at high pH levels while Ca^{2+} had a small effect on adsorption

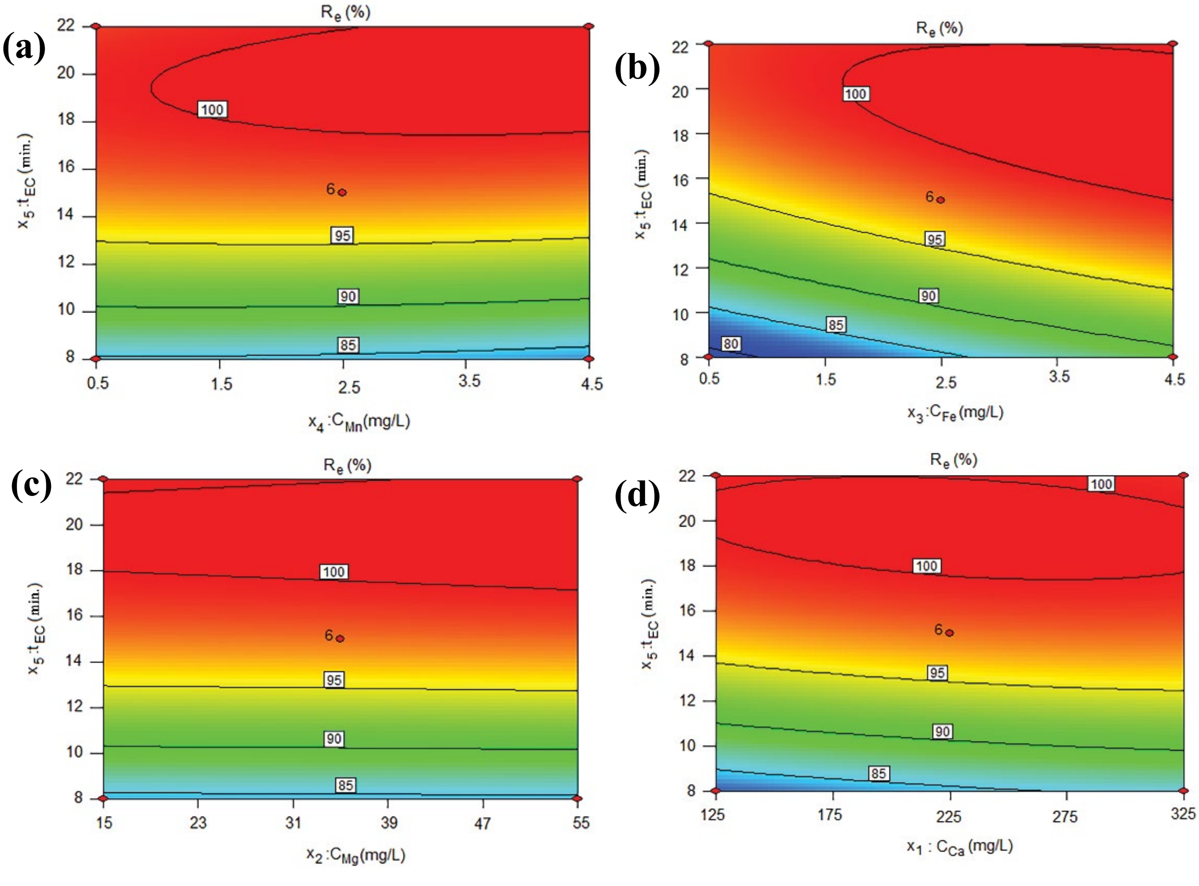

Fig. 2. Contour plots showing the effects of (a) x_4:C_{Mn} and x_5:t_{EC}, (b) x_3:C_{Fe} and x_5:t_{EC}, (c) x_2:C_{Mg} and x_5:t_{EC}, and (d) x_1:C_{Ca} and x_5:t_{EC} on percentage of As(V) removal.

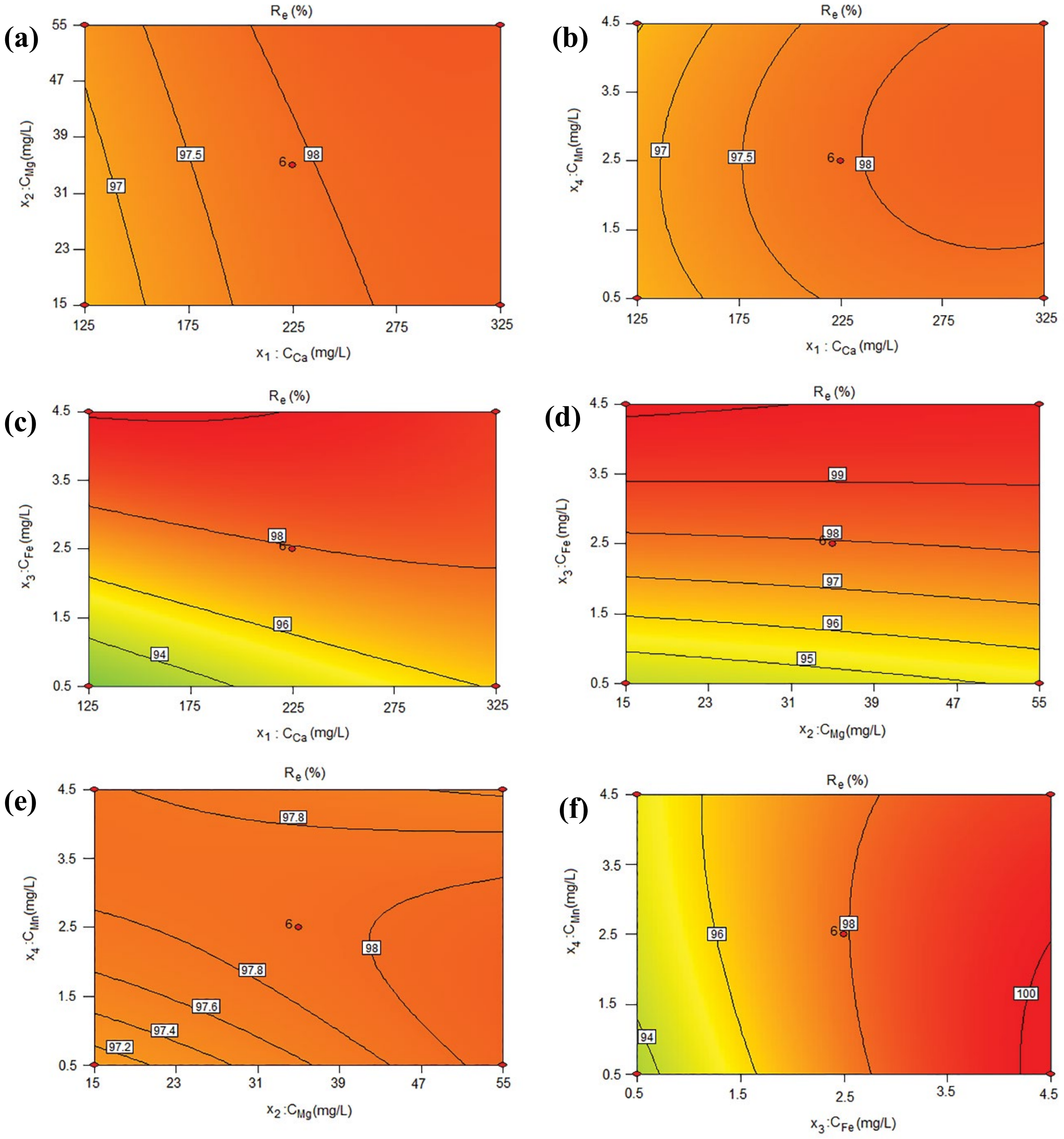

Fig. 3. Contour plots showing the effects of (a) x_1:C_{Ca} and x_2:C_{Mg}, (b) x_1:C_{Ca} and x_4:C_{Mn}, (c) x_1:C_{Ca} and x_3:C_{Fe}, (d) x_2:C_{Mg} and x_3:C_{Fe}, (e) x_2:C_{Mg} and x_4:C_{Mn}, and (f) x_3:C_{Fe} and x_4:C_{Mn} on percentage of As(V) removal.

of As(III) at pH 3–11 [40]. Arsenic ions from groundwater were removed through adsorption processes onto produced aluminum hydroxides flocs, surface complexation reactions with aluminum hydroxides and co-precipitation reactions with calcium-magnesium-aluminum hydroxides flocs and aluminum hydroxides flocs by electrochemically generated Al^{3+} ions and hydrolyzed solution reactions [41]. Therefore, cations such as Ca^{2+} and Mg^{2+} may enhance the arsenate removal with the formation of (Ca, Mg)-aluminum-arsenate-hydroxide; [Ca, Mg]$Al_n(OH)_{(3n-1)}(AsO_4)_{(s)}$ and co-precipitate in the EC process [23,42]. The possible reaction may be expressed in Eq. (13)

$$nAl^{3+} + 3nOH^- + HAsO_4^{2-} + \left[Ca^{2+} \text{or } Mg^{2+}\right] \rightarrow \left[Ca \text{ or } Mg\right]Al_n\left(OH\right)_{(3n-1)}\left(AsO_4\right) + H_2O \quad (13)$$

It is possible to remove arsenic using only calcium and magnesium ions which form calcium arsenate ($Ca_3(AsO_4)_{2(s)}$), calcium-magnesium arsenate hydroxide or arsenate hydroxyl precipitates. However, the pH adjustment is required for calcium-magnesium arsenate precipitation because $Ca_3(AsO_4)_{2(s)}$ precipitates are soluble at neutral pH while the As(V) is mainly found as $HAsO_4^{2-}$ or $H_2AsO_4^-$ forms under pH 11. The pH fluctuations can be eliminated and solubility of arsenate species from the decrease of pH by the hydrolysis of metal salts can be prevented in the EC process. Magnesium has also significant impacts on precipitate formation and arsenic removal. In the EC process, arsenic removal may result in co-precipitation with magnesium hydroxide flocks. However, high concentrations of magnesium have a negative effect on arsenic removal due to the inhibition of coagulant formation while an appropriate amount of magnesium has a positive effect on arsenic removal [43]. Also, high concentrations of Ca^{2+} and Mg^{2+} ions cause a notable negative effect on arsenic removal because of the passivation of the electrode surface.

The arsenic removal efficiency enhances with increasing Ca^{2+} concentration. Fig. 2c demonstrates the effect of Ca^{2+} concentration on arsenate removal. At the minimum Ca^{2+} concentration of 125 mg/L arsenic removal efficiency was observed as almost 94%, while the arsenic removal efficiency was found almost 98% at the maximum Ca^{2+} concentration of 325 mg/L. When the other cations remained constant, arsenic removal efficiency increased from 91.03% (C_f of 17.95 μg/L) to 95.77% (C_f of 8.46 μg/L) at 125 and 325 mg/L Ca^{2+} concentrations, respectively (runs 7 and 32, in Table 2. Similarly, the removal efficiency trend was found as 97.02% and 98.40% for Ca^{2+} concentrations of 125 and 325 mg/L, respectively (runs 6 and 17). The final pHs of all experimental runs were measured as almost neutral (Table 3). Therefore, it can be concluded that the main arsenic removal mechanism may be $Ca_3(AsO_4)_{2(s)}$ precipitation due to the neutral pH of the solution. However, the residual Ca^{2+} concentration was too high at the end of the treatment due to the low stability constants for the complexation of Ca^{2+} compared to other cations by hydroxyl (Table 2). The arsenic removal efficiency at three different Ca^{2+} concentrations also improved with the increase in EC time (Fig. 2d). For instance, the removal efficiency of arsenic for 225 mg/L initial calcium concentration was found at almost 85% and 95% at 8–18 min, respectively. The similar trends were observed for the Ca^{2+} concentration of 125 and 325 mg/L. The removal efficiency was 98% for 225 mg/L of calcium concentration at 2.5 mg/L of iron dosage when the removal efficiency decreased to 96% at 1.5 mg/L of iron dosage (Fig. 3c). In addition, the removal efficiency was found as 98% for 325 mg/L of calcium concentration at 1.5 mg/L of manganese dosage when the removal efficiency decreased to almost 97.5% at 2.5 mg/L of manganese dosage (Fig. 3b). On the other hand, arsenate removal efficiency was observed to be 99.69% for 225 mg/L of calcium concentration at 15 mg/L magnesium concentration while the removal efficiency decreased to 98.35% at 55 mg/L magnesium concentration due to the negative interaction between calcium and magnesium cations (runs 2 and 26). Arsenic adsorption capacity was calculated as 20.32 μg As/mg Al for 325 mg/L of calcium and 19.45 μg As/mg Al for 125 mg/L of calcium, respectively. The OC also decreased with the increment of the calcium concentration. The OC was calculated as 0.127 \$/m^3 for 325 mg/L and 0.332 \$/m^3 for 125 mg/L calcium concentration (runs 7 and 32, Table 3). A similar behavior was observed for runs 6 and 17.

The positive effect of magnesium on the removal efficiency can be interpreted in Tables 2 and 3. Arsenic removal efficiency was found as 98.04% at magnesium concentration of 55 mg/L while the removal efficiency was 97.99% at 15 mg/L magnesium content (runs 20 and 21). Similarly, the removal efficiency increased from 97.37% at magnesium concentration of 15 mg/L to 99.94% at 55 mg/L (runs 13 and 16). Similarly, the removal efficiency was 97.99% at 15 mg/L while the removal efficiency was 98.04% at 55 mg/L magnesium concentration. The arsenic adsorption capacity increased with the increase in magnesium concentrations. At 55 and 15 mg/L magnesium concentrations, arsenic adsorption capacity was found as 12.48 μg As/mg Al and 12.45 μg As/mg Al, respectively. However, the results showed that the increase in arsenic adsorption capacity was not significant. The OC was calculated as 0.086 \$/m^3 for 55 mg/L and 0.104 \$/m^3 for 15 mg/L magnesium concentration (runs 20 and 21).

4.3. Effects of iron and manganese on arsenic removal

At the beginning of the EC process, the iron competes with arsenic for adsorption sites of aluminum flocs. However, as the EC process proceeds the iron hydroxide generation and precipitation become more predominant, there formed unused adsorption sites for arsenic. That is, the presence of iron increases the arsenic removal rate by the EC process [32]. In the EC process, the possible reactions between the iron hydroxide complexes and arsenic species were presented in the following equations.

$$Fe^{2+} + 3OH^- \rightarrow FeOOH_{(s)} + H_2O + e^- \tag{14}$$

$$3FeOOH_{(s)} + HAsO_4^{2-} \rightarrow \left(FeO\right)_3 AsO_{4(s)} + H_2O + 2OH^- \tag{15}$$

$$2FeOOH_{(s)} + H_2AsO_4^- \rightarrow \left(FeO\right)_2 HAsO_{4(s)} + H_2O + OH^- \tag{16}$$

The removal efficiency for 0.5 and 4.5 mg/L iron concentration was found as 95.47% (C_f of 9.07 μg/L) and 98.35% (C_f of 3.31 μg/L) at operating time of 15 min, respectively (runs 26 and 35). The same trend was observed for the runs 7 and 25 as 95.77% (C_f of 8.46 μg/L) at 0.5 mg/L iron and 99.44% (C_f of 1.12 μg/L) at 4.5 mg/L iron concentration. The recommended limit value of arsenic (<10 μg/L) was met in cases of low (0.5 mg/L) and high (4.5 mg/L) iron concentrations. $Fe(OH)_x$ species also increased with the increase in iron concentration and operating time. Arsenic removal efficiency increased from 81.63% (C_f of 36.75 μg/L) at 8 min to 100% (C_f of 0 μg/L) at 22 (runs 5 and 42). A similar trend is observed in Fig. 1b, arsenic removal efficiency increased from 80% at 8 min to 100% at 22 min for 2.5 mg/L iron concentration. It was observed that there were enough monomeric and polymeric iron hydroxides species as well as aluminum hydroxide species in the EC process to remove arsenic at operating time of 22 min and the increase in the iron hydroxide species with increase in operating time improved the removal efficiency at the same experimental runs. However, the increasing operating time increases the OC, energy consumption, and amount of sludge formation. For instance, at 2.5 mg/L iron concentration the OC, energy consumption, and amount of sludge formation were 0.055–0.130 \$/m^3, 0.2213–0.6469 kWh/m^3, and 0.0089–0.0231 kg/m^3 for 8 and 22 min, respectively.

Arsenic removal efficiency varied from 82.83% (C_f of 34.35 μg/L) to 85.05% (C_f of 29.9 μg/L) at 8 min (runs 4 and 34) and the effluent concentrations were >10 μg/L. It was observed that there weren't enough monomeric and polymeric aluminum hydroxyl species and manganese oxide/hydroxide species in the EC process, which enhances the arsenic removal efficiency. At pH 3, the form of aluminum mainly exists as monomeric species, like $Al(OH)^{2+}$ and $Al(OH)_2^+$. With the initial pH kept in the range of 4–8, polymeric aluminum species formed at the cathode and precipitated $Al(OH)_3$ species accelerated the removal of pollutants. According to literature, the manganese hydroxide precipitation at the cathode occurs at pH ~ 7–8 [44]. Tomohito et al. [45], have also reported that the surfaces of Mn_3O_4 and $Mn(OH)_2$ were charged positively at a pH of 6–10. Within this pH range, the adsorption of H_2AsO_4 and $HAsO_4^{2-}$ onto Mn_3O_4 and $Mn(OH)_2$ with electrostatic interaction was observed. Thus, it can be interpreted that the selected pH of 7.5 was appropriate for significant arsenic removal in the present paper. According to the present study, the increment in As(III) removal caused by manganese was mainly due to As(III) oxidation to As(V) by manganese oxide. Furthermore, the adsorption of As(V) by Mn_3O_4 and $Mn(OH)_2$ surface can play a significant role in enhancing arsenic removal.

Arsenic removal efficiency can positively influence manganese species due to its ability to adsorb/coprecipitate As(V) on manganese dioxide (MnO_2) and manganese hydroxide ($Mn(OH)_2$) surfaces. During EC, increased quantities of OH^- were produced with applied current and O_2 supplied by airflow. Thus, Mn^{2+} ions were transformed to $Mn(OH)_2$ and followed by the formation of $Mn(OH)_2$ to MnO_2 by O_2 (Eqs. (17) and (18)). Manganese oxides increase the As(III) oxidation ratio and increase the adsorption of As(V). The release of Mn ions from manganese oxide caused by As(III) oxidation may increase its surface area, which increases the exposure of more active sites for arsenic immobilization [46].

$$Mn^{2+} + 2OH^- \rightarrow Mn\left(OH\right)_{2(s)} \tag{17}$$

$$2Mn\left(OH\right)_{2(s)} + O_{2(g)} \rightarrow 2MnO_{2(s)} + 2H_2O \tag{18}$$

Arsenic removal efficiency increased from 97.45% (C_f of 5.10 μg/L) to 98.40% (C_f of 3.21 μg/L) at 0.5 and 4.5 mg/L Mn^{2+} concentrations, respectively (runs 6 and 22, Table 2). Removal efficiencies of the other cations at 0.5–4.5 mg/L of Mn^{2+} were obtained as 1.11 and 1.29% for Ca^{2+}, 2.29 and 5.14% for Mg^{2+}, 16.4 and 45.6% for Fe^{2+}, respectively. The results indicated that almost 2 times more cation removal was achieved at high Mn^{2+} concentration. A similar result was obtained for the removal as 99.51% at 0.5 mg/L of Mn^{2+} and 99.65% at 4.5 mg/L of Mn^{2+} (runs 36 and 37). The coprecipitation of the $Mg(OH)_2$, $Mn(OH)_2$ and $Fe(OH)_2$ could have played a significant role in the removal mechanism [44]. The stability constants for complexation of Ca^{2+}, Mg^{2+}, and Fe^{2+} by hydroxyl are 1.40, 2.21 and 4.50, respectively [47]. Therefore, it can be concluded that under the same conditions, Fe^{2+} ions could be removed more quickly than the other cations. The removal efficiency was found as 98% for 4.5 mg/L of manganese concentration at 2.5 mg/L of iron dosage when the removal efficiency decreased to almost 95% for 2.5 mg/L of manganese concentration. For instance, it could be also seen from Table 1. that the removal efficiency at constant iron concentration of 2.5 mg/L increased from 99.22% for 0.5 mg/L of manganese concentration to 99.53% for 4.5 mg/L of manganese concentration (runs 19 and 28). Also, final pHs for the initial manganese concentration of 0.5–4.5 mg/L were measured as 6.9 and 6.74, respectively (Table 3). The removal efficiency of As(V) also increased with the increasing operating time. At manganese concentration of 2.5 mg/L, As(V) removal efficiency was found as almost 90% at operating time of 12 min, while the removal efficiency of 100% was observed at operating time of 18 min (Fig. 1a). Arsenic adsorption capacity per mg Al was calculated as 8.60 μg As/mg Al for 0.5 mg/L of manganese and 8.62 μg As/mg Al for 4.5 mg/L of manganese, respectively (Table 3). The electrode and energy consumption for 0.5 and 4.5 mg/L of manganese concentrations were determined as 0.0083 kg/m^3–0.8326 kWh/m^3 and 0.0078 kg/m^3–0.8312 kWh/m^3, respectively. The OC also decreased from 0.202 \$/m^3 at 0.5 mg/L of manganese concentration to 0.199 \$/m^3 at 4.5 mg/L of manganese concentrations with respect to energy and ELC. It was obvious that there is a slight change in OC, electrode and energy consumption in 0.5 and 4.5 mg/L of manganese concentration. However, the results indicated that the increment of manganese concentration decreases the OC, ENC, and ELC of the EC process. The OC were calculated for some arsenic treatment process such as 0.357 \$/m^3 at initial arsenite concentration of 500 μg/L for batch EC using Al plate electrodes, 0.52 \$/m^3 at 100 μg As(V)/L for reverse osmosis, 4,850 \$/lb at 100 μg As/L for adsorption using nano-scale zero-valent iron, 3.40 \$/m^3 for ion-exchange, 1.21 \$/m^3 for coagulation–filtration and 1.20 \$/m^3 for granulated ferric hydroxide/oxide [19].

4.4. Effects of operating time on arsenic removal

The EC time is one of the most important parameters controlling the formation of coagulant within an EC process. According to Faraday's law in Eq. (10), these parameters determine the amount of production coagulant (Al^{3+} for Al anodes and Fe^{2+} for Fe anodes) and the size of the $H_{2(g)}$ bubble production. Considering these results, the operating time was observed to have a significant positive effect on arsenic removal efficiency. As shown in Fig. 2, arsenic removal efficiency increased with the increment of operating time for all cations. The arsenic removal efficiency increased from 85% at 8 min to 100% at 18 min for 2.5 mg/L manganese concentration (Fig. 2a). Similarly, removal efficiency increased from 85% at 8 min to 99.99% for 225 mg/L calcium concentration. For instance, EC time from 8 to 22 min and arsenic removal efficiency increased from 90.6% to 99.98% at C_{Ca} of 225 mg/L, C_{Mg} of 35 mg/L, C_{Fe} of 4.5 mg/L and C_{Mn} of 2.5 mg/L (exp. runs 8 and 31, Table 2). Overall, interactions of operating time with the cations on the arsenic removal efficiency showed that the removal efficiency increased with the increase in operating time. The aluminum hydroxide formation and complex reactions by cations could be increased with an increase in EC time. Arsenic adsorption capacity (q_e) was another aspect. The dissolved amount of Al increased with operating time while the amount of removed arsenic decreased with per mg Al dosage. For instance, values of q_e and per mg Al dosage were 20.26 µg As/mg Al or 1.89 µg As/C and 6.71 at 8 min and 8.60 µg As/mg Al or 0.80 µg As/C and 18.45 at operating time of 22 min, respectively (exp. runs 19 and 34) as shown in Table 3. A similar trend was observed for exp. runs 27 and 46. Also, the OC, amount of sludge formation, and ELC increased with an increase in EC time. At 8 and 22 min of operating time, the OC, amount of sludge formation, and ELC were found as 0.112–0.272 \$/m^3, 0.0084–0.0231 kg/m^3, and 0.0066–0.0096 kg/m^3, respectively (exp. runs 5 and 42). As a result, operating time in the EC reactor using ball Al anodes was found to be the most important parameter on arsenic removal.

4.5. Comparison of the obtained results with literature

Table 4 shows a comparison of the findings of this study and earlier studies in the literature in terms of treatment

Table 4
Comparison of the obtained results with literature studies

Treatment process and water type	Examined cations	Operating conditions	Arsenic removal efficiency (%)	References
$KMnO_4$–Fe(II) process and synthetic water (SW)	Ca^{2+}	Permanganate dosage: 18.6 µM, Ca^{2+} concentration: 2.5 mM, pH: 7–9, C_0: 13.3 mM As(III), and t_{EC}: 30 min	≈85%	[53]
Electrocoagulation and SW	Ca^{2+}	Electrode type: Al plate, stirring speed: 400 rpm, I = 0.6 A, reaction time = 40 min, energy consumption: 7.8 kJ, C_0: 20 mM As(V), and Ca^{2+} concentration: 20 mM	≈80%	[49]
$FeCl_3$ coagulation and SW	Ca^{2+}	Ca^{2+} concentration: 80 mg L^{-1}, t_{EC}: 30 min, As/Fe molar ratio: 0.35, HA concentration: 5 mg/L, and C_0: 7.5 mg/L As(V) and As(III)	60% (As(III)) 90% (As(V))	[51]
Reclaimed iron-oxide coated sand (RIOCS) adsorption and SW	Ca^{2+}	C_0: 500 µg/L As(V), stirring speed: 100 rpm, reaction time: 24 h, RIOCS dosage: 24 g/L, temperature = 25°C, Ca^{2+} concentration: 150 mg L^{-1}, and pH: 7	>90%	[54]
Aluminum oxides adsorption and SW	Ca^{2+}	Adsorbent dosage: 2 g/L, C_0: 5×10^{-4} M As(V), pH: 3, and Ca^{2+} concentration: 5×10^{-4} M	90%	[23]
Electrocoagulation process and SW	Fe^{2+}	I = 12.5 A m^{-2}, $C_{As,0}$: 4 mg L^{-1}, reaction time: 10 min, Fe^{2+} concentration: 25 mg/L, pH: 6.2, stirring speed: 200 rpm, and electrode type: Al plate	>90%	[50]
Electrocoagulation and SW	Mg^{2+}	Mg^{2+} concentration: 10 mg/L, reaction time: 30 min, I = 0.1 A, pH: 7, $C_{As,0}$: 1 mg/L As(III), and electrode type: Fe plate	>90%	[43]
Nano zero-valent iron process and SW	Ca^{2+}	$C_{As,0}$: 1,000 µg/L, pH: 7.9, NZVI = 0.023 g/L, Ca^{2+} concentration: 500 mg/L, and reaction time: 40 min	>90% (As(III)) >90% (As(V))	[55]
Nano zero-valent iron process and SW	Ca^{2+}	$C_{As,0}$: 2 mg/L As(V), pH: 9.17, Ca^{2+} concentration: 32 mg/L, reaction time: 60 min, Fe^0 dosage: 0.1 g, and HCO_3: 3 mM	>90%	[56]
Lepidocrocite adsorption and SW	Fe^{2+}	$C_{As,0}$: 500 µg/L As(III), pH: 5.6, Fe^{2+} concentration: 90 µM, reaction time: 50 h, stirring speed: 300 rpm, and lepidocrocite stock suspension: 6 g/L	93.08%	[57]
Coagulation–Floculation and groundwater (GW)	Ca^{2+}, Mg^{2+}	$C_{As,0}$: 500 µg/L As(III), Ca^{2+} concentration: 40 mg/L, Mg^{2+} concentration: 24 mg/L, reaction time: 60 min, pH: 7.31, Si concentration: 5.9, and HCO_3 concentration: 196 mg/L	≈58% (Ca^{2+} addition) ≈60% (Mg^{2+} addition)	[58]
$FeCl_3$ coagulation and SW	Ca^{2+}	$C_{As,0}$: 2.36 µg/L As(III) and As(V), $FeCl_3$ dosage: 4.37 mg/L, reaction time: 30 min, Ca^{2+} concentration: 5.2 mg/L, and pH: 6	100% (As(V)) ≈30% (As(III))	[52]
Forward osmosis and SW	Ca^{2+}, Mg^{2+}	$C_{As,0}$: 30 mg/L As(V), pH: 7, Ca^{2+} concentration: 150 mg/L, Mg^{2+} concentration: 150 mg/L, and reaction time: 2 h	87.5% (Ca^{2+} addition) 89.5% (Mg^{2+} addition)	[59]

processes, arsenic species and concentrations, and cation species. It was clear from Table 4 that the combined effect of cations (Ca^{2+}, Mg^{2+}, Mn^{2+}, and Fe^{2+}) did not refer to any treatment process. Commonly, the single effect of Ca^{2+}, Mg^{2+}, and Fe^{2+} was investigated.

The removal efficiencies of 60%–100% were observed for As(V) or As(III) in the range of 7.5–30 mg/L. The removal efficiencies were found as approximately 58% and 65% at initial arsenic concentration of 500 μg/L as As(III) with Ca^{2+} (40 mg/L as Ca^{2+}) and Mg^{2+} (24 mg/L as Mg^{2+}) addition, respectively [48]. The results from the present study revealed that there is a serious gap in the investigation of the effects of cations on arsenic removal in the literature. Therefore, this study not only contributes to fill this gap in the literature but also proves the efficiency of air-injected EC process on arsenic removal. Arsenic was removed about 80% at the optimum operating conditions (applied current of 0.6 A, EC time of 40 min, and stirring speed of 400 rpm) in EC process using Al plate electrode when As(V) and Ca^{2+}concentations were 1,500 and 800 mg/L in the simulated solution [49]. At arsenic concentration of 4 mg/L and iron concentration of 25 mg/L in synthetic solution, arsenic removal efficiency of EC reactor using Al plate anodes was >90% at initial pH 6.2, i = 12.5 A/m^2 and 10 min [50]. At As(III) concentration of 1 mg/L and Mg^{2+} concentration of 10 mg/L in synthetic solution, the removal efficiency by Fe plate anodes was >90% at, reaction time of 30 min, initial pH of 7 and applied current of 0.1 A [43]. Arsenic (V) adsorption capacity of aluminum oxides and removal efficiency was 16.7 mg/g and 90% at initial pH of 3, adsorbent dosage of 2 g/L, initial As(V) concentration of ~37 mg/L and Ca^{2+} concentration of 20 mg/L [23]. As(V) and As(III) by $FeCl_3$ coagulation were 90% and 60% at Ca^{2+} concentration of 80 mg/L, operating time of 30 min, As/Fe molar ratio of 0.35, humic acid concentration of 5 mg/L, and As(V) and As(III) concentrations of 7.5 mg/L [51,52] found that As(V) and As(III) removal by ferric coagulation was 100% and 30% at As(III) and As(V) concentrations of 2.36 μg/L, $FeCl_3$ dosage of 4.37 mg/L, reaction time of 30 min, Ca^{2+} concentration of 5.2 mg/L and pH: 6. In a conventional groundwater treatment plant, separate reactors are needed for arsenic and hardness removal, which in turn leads to an increase in both investment and OC. OC for the arsenic removals meeting the permissible WHO value were 1.21 $/m³ for coagulation–filtration, 1.20 $/m³ for granulated ferric hydroxide/oxide, 3.20 $/m³ for activated alumina, 3.40 $/m³ for ion exchange, 3.72 $/m³ for reverse osmosis and 0.054 $/m³ for combined arsenic and iron removal by air oxidation–filtration, respectively [19]. However, the OC for the arsenic and hardness removal in the air injection EC process was calculated as 0.03318 $/m³ which was more economical compared to the literature values.

5. Conclusions

In the present study, forty-six experiments were carried out by the BBD in the air-injected EC process for the investigation of the effects of cations on arsenic removal. The effect of cations and operating time were considered. There was a positive effect of operating time on the arsenic removal efficiency. Likewise, arsenic removal efficiency increased with the increasing concentrations of iron, magnesium, calcium, and manganese. The combined interactions of independent variables didn't have a significant effect on arsenic removal. Consequently, the maximum R_e, q_e and minimum OC at 16.85 min of operating time were 99.9%, 11.14 μgAs/mg Al, and 0.03318 $/m³ when concentrations of calcium, magnesium, iron, and manganese were 305, 42, 3.3, and 2.34 mg/L, respectively. The results indicated that the air-injected EC reactor is a promising treatment process for effective arsenic removal from groundwater including cations.

Symbols

α — Electrical energy price, $/kWh
β — Al electrode price, $/kg
U — Voltage, V
i — Applied current, A
t_{EC} — EC time, min
v — Volume of the arsenic-contaminated groundwater in the air-injection EC reactor, m^3
M_{Al} — Molecular weight of the Al, g/mol
z — Number of electrons
F — Faraday's constant, C/mol
q — Charge loading, Coulomb
C_i — Initial arsenic concentrations, μg/L
C_t — Arsenic concentrations at time of t, μg/L

Acknowledgment

The authors would like to express their appreciation for the financial support of TUBITAK (The Scientific and Technical Research Council of Turkey, Project Number = 111Y103).

References

[1] P. Ravenscroft, H. Brammer, K. Richards, Arsenic Pollution: A Global Synthesis RGS IBG Book Series, A John Wiley & Sons Publication Ltd., London, 2009.

[2] C.M. Steinmaus, C. Ferreccio, J.A. Romo, Y. Yuan, S. Cortes, G. Marshall, L.E. Moore, J.R. Balmes, J. Liaw, T. Golden, A.H. Smith, Drinking water arsenic in Northern Chile: high cancer risks 40 years after exposure cessation, Cancer Epidemiol. Biomarkers Prev., 22 (2013) 623–630.

[3] S.-W. Wang, Y.-M. Kuo, Y.-H. Kao, C.-S. Jang, S.K. Maji, F.-J. Chang, C.-W. Liu, Influence of hydrological and hydrogeochemical parameters on arsenic variation in shallow groundwater of southwestern Taiwan, J. Hydrol., 408 (2011) 286–295.

[4] O. Gunduz, A. Baba, H. Elpit, Arsenic in Groundwater in Western Anatolia, Turkey, A review: Groundwater Quality Sustainability, CRC Press, Boca Raton 2012, pp. 141–149.

[5] P. Mondal, S. Bhowmick, D. Chatterjee, A. Figoli, B.V. der Bruggen, Remediation of inorganic arsenic in groundwater for safe water supply: a critical assessment of technological solutions, Chemosphere, 92 (2013) 157–170.

[6] M.M. Rahman, J.C. Ng, R. Naidu, Chronic exposure of arsenic via drinking water and its adverse health impacts on humans, Environ. Geochem. Health, 31 (2009) 189–200.

[7] World Health Organization, Guidelines for Drinking Water Quality, 3rd ed., Vol. 1, WHO Press, Switzerland-Geneva, 2004.

[8] US-EPA (United States Environmental Protection Agency), Implementation Guidance for the Arsenic Rule, Environmental Protection Agency, Government Printing Office, Washington, 2002.

[9] US-EPA (United States Environmental Protection Agency), Technologies and Costs for Removal of Arsenic from Drinking Water, Government Printing Office, Washington, D.C., 2000.

[10] M.R. Awual, Assessing of lead(III) capturing from contaminated wastewater using ligand doped conjugate adsorbent, Chem. Eng. J., 289 (2016) 65–73.

[11] M.R. Awual, M. Khraisheh, N.H. Alharthi, M. Luqman, A. Islam, M.R. Karim, M.M. Rahman, A. Khaleque, Efficient detection and adsorption of cadmium(II) ions using innovative nano-composite materials, Chem. Eng. J., 343 (2018) 118–127.

[12] M.R. Awual, Y. Miyazaki, T. Taguchi, H. Shiwaku, T. Yaita, Encapsulation of cesium from contaminated water with highly selective facial organic–inorganic mesoporous hybrid adsorbent, Chem. Eng. J., 291 (2016) 128–137.

[13] A. Shahat, M.R. Awual, M.A. Khaleque, M.Z. Alam, M. Naushad, A.M.S. Chowdhury, Large-pore diameter nano-adsorbent and its application for rapid lead(II) detection and removal from aqueous media, Chem. Eng. J., 273 (2015) 286–295.

[14] M.R. Awual, New type mesoporous conjugate material for selective optical copper(II) ions monitoring & removal from polluted waters, Chem. Eng. J., 307 (2017) 85–94.

[15] M.R. Awual, Novel nanocomposite materials for efficient and selective mercury ions capturing from wastewater, Chem. Eng. J., 307 (2017) 456–465.

[16] M.R. Awual, A novel facial composite adsorbent for enhanced copper(II) detection and removal from wastewater, Chem. Eng. J., 266 (2015) 368–375.

[17] M.R. Awual, Solid phase sensitive palladium(II) ions detection and recovery using ligand based efficient conjugate nanomaterials, Chem. Eng. J., 300 (2016) 264–272.

[18] M.R. Awual, I.M.M. Rahman, T. Yaita, M.A. Khaleque, M. Ferdows, pH dependent Cu(II) and Pd(II) ions detection and removal from aqueous media by an efficient mesoporous adsorbent, Chem. Eng. J., 236 (2014) 100–109.

[19] E. Şık, E. Demirbaş, A.Y. Goren, M.S. Oncel, M. Kobya, Arsenite and arsenate removals from groundwater by electrocoagulation using iron ball anodes: Influence of operating parameters, J. Water Process Eng., 18 (2017) 83–91.

[20] S. Amrose, S.R.S. Bandaru, C. Delaire, C.M. Genuchten, A. Dutta, A. DebSarkar, C. Orr, J. Roy, A. Das, A.J. Gadgil, Electro-chemical arsenic remediation: field trials in West Bengal, Sci. Total Environ., 488–489 (2014) 539–546.

[21] M. Kobya, F. Ozyonar, E. Demirbas, E. Şık, M.S. Oncel, Arsenic removal from groundwater of Sivas-Şarkişla Plain, Turkey by electrocoagulation process: comparing with iron plate and ball electrodes, J. Environ. Chem. Eng., 3 (2015) 1096–1106.

[22] R. Alcacio, J.L. Nava, G. Carreno, E. Elorza, F. Martinez, Removal of arsenic from deep well by electrocoagulation in a continuous filter press reactor, Water Sci. Technol. Water Supply, 14 (2014) 189–195.

[23] J.K. Yang, Y.J. Park, K.H. Kim, H.Y. Lee, K.C. Min, S.M. Lee, Effect of co-existing copper and calcium on the removal of As(V) by reused aluminum oxides, Water Sci. Technol., 67 (2013) 187–192.

[24] D. Laky, I. Liscko, Arsenic removal by ferric-chloride coagulation-effect of phosphate, bicarbonate and silicate, Water Sci. Technol., 64 (2011) 1046–1055.

[25] M.R. Awual, M.A. Hossain, M.A. Shenashen, T. Yaita, S. Suzuki, A. Jyo, Evaluating of arsenic(V) removal from water by weak-base anion exchange adsorbents, Environ. Sci. Pollut. Res., 20 (2013) 421–430.

[26] M.R. Awual, A. Jyo, Rapid column-mode removal of arsenate from water by crosslinked poly(allylamine) resin, Water Res., 43 (2009) 1229–1236.

[27] M.R. Awual, S.A. El-Safty, A. Jyo, Removal of trace arsenic(V) and phosphate from water by a highly selective ligand exchange adsorbent, J. Environ. Sci., 23 (2011) 1947–1954.

[28] M.R. Awual, M.A. Shenashen, T. Yaita, H. Shiwaku, A. Jyo, Efficient arsenic(V) removal from water by ligand exchange fibrous adsorbent, Water Res., 46 (2012) 5541–5550.

[29] M. Kobya, E. Demirbas, O.T. Can, M. Bayramoglu, Treatment of levafix orange textile dye solution by electrocoagulation, J. Hazard. Mater., 132 (2006) 183–188.

[30] A.Y. Gören, M.S. Öncel, E. Demirbas, E. Şık, M. Kobya, Removal of arsenate by EC reactor using Al ball anode electrodes, Water Pract. Technol., 13 (2018) 753–763.

[31] E. Şık, M. Kobya, E. Demirbaş, M.S. Oncel, A.Y. Goren, Removal of As(V) from groundwater by a new electrocoagulation reactor using Fe ball anodes: optimization of operating parameters, Desal. Wat. Treat., 56 (2015) 1177–1190.

[32] M.Y.A. Mollah, R. Schennach, J.P. Parga, D.L. Cocke, Electrocoagulation (EC)-science and applications, J. Hazard. Mater., 84 (2001) 29–41.

[33] M. Rebhun, M. Lurie, Control of organic matter by coagulation and floc separation, Water Sci. Technol., 27 (1993) 1–20.

[34] X. Chen, G. Chen, P.L. Yue, Separation of pollutants from restaurant wastewater by electrocoagulation, Sep. Purif. Technol., 19 (2000) 65–76.

[35] S.S. Tripathy, A.M. Raichur, Enhanced adsorption capacity of activated alumina by impregnation with alum for removal of As(V) from water, Chem. Eng. J., 138 (2008) 179–186.

[36] T.S. Singh, K.K. Pant, A Comparative Study for the Removal of As(III) and As(V) by Activated Alumina, Natural Arsenic in Groundwater: Occurrences, Remediation and Management, Taylor and Francis Series, Balkema Publications, The Netherlands, 2004.

[37] P.K. Roy, A. Majumder, G. Banerjee, M.B. Roy, S. Pal, A. Mazumdar, Removal of arsenic from drinking water using dual treatment process, Clean Technol. Environ. Policy, 17 (2015) 1065–1076.

[38] APHA (American Public Health Association), Standard Methods for the Examination of Water and Wastewater, 19th ed., American Public Health Association, Washington, D.C., 1998.

[39] R.H. Myers, D.C. Montgomery, Response Surface Methodology: Process and Product Optimization Using Designed Experiments, John Wiley and Sons, New York, 2002.

[40] M. Kanematsu, T.M. Young, K. Fukushi, P.G. Green, J.L. Darby, Arsenic (III, V) adsorption on a goethite-based adsorbent in the presence of major co-existing ions: modeling competitive adsorption consistent with spectroscopic and molecular evidence, Geochim. Cosmochim. Acta, 106 (2013) 404–428.

[41] V. Pallier, G.F. Cathalifaud, B. Serpaud, Influence of organic matter on arsenic removal by continuous flow electrocoagulation treatment of weakly mineralized waters, Chemosphere, 8 (2011) 21–28.

[42] D.H. Moed, D. van Halem, J.Q.J.C. Verberk, G.L. Amy, J.C. van Dijk, Influence of groundwater composition on subsurface iron and arsenic removal, Water Sci. Technol., 66 (2012) 173–178.

[43] H.J. You, I.S. Han, Effects of dissolved ions and natural organic matter on electrocoagulation of As(III) in groundwater, J. Environ. Chem. Eng., 4 (2016) 1008–1016.

[44] A. Shafaei, M. Rezayee, M. Arami, M. Nikazar, Removal of Mn^{2+} ions from synthetic wastewater by electrocoagulation process, Desalination, 260 (2010) 23–28.

[45] K. Tomohito, S. Youhei, Y. Toshiaki, Removal of arsenic from an aqueous solution by co-precipitation with manganese oxide, J. Environ. Chem. Eng., 2 (2014) 2045–2049.

[46] J. Hou, J. Luo, S. Song, Y. Li, Q. Lid, The remarkable effect of the coexisting arsenite and arsenate species ratios on arsenic removal by manganese oxide, Chem. Eng. J., 315 (2017) 159–166.

[47] M.M. Benjamin, Water Chemistry, McGraw-Hill Series in Water Resources and Environmental Engineering, New York, 2002, pp. 362–464.

[48] R. De, T.S.C.M. Wetering, D. Dijk, D. Halem, Influence of HPO_4^{2-}, H_4SiO_4,Ca^{2+},Mg^{2+}on Fe floc growth and As(III) removal in aerated, natural groundwater, J. Water Process Eng., 25 (2018) 149–156.

[49] C.Y. Hu, S.L. Lo, W.H. Kuan, High concentration of arsenate removal by electrocoagulation with calcium, Sep. Purif. Technol., 126 (2014) 7–14.

[50] J.F.A. Silva, N.S. Graça, A.M. Ribeiro, A.E. Rodrigues, Electrocoagulation process for the removal of co-existent fluoride, arsenic and iron from contaminated drinking water, Sep. Purif. Technol., 197 (2018) 237–243.

[51] Y. Kong, J. Kang, J. Shen, Z. Chen, L. Fan, Influence of humic acid on the removal of arsenate and arsenic by ferric chloride: effects of pH, As/Fe ratio, initial As concentration, and co-existing solutes, Environ. Sci. Pollut. Res. Int., 24 (2017) 2381–2393.

[52] J. Qiao, Z. Jiang, B. Sun, Y. Sun, Q. Wang, X. Guan, Arsenate and arsenite removal by $FeCl_3$: effects of pH, As/Fe ratio, initial As concentration and co-existing solutes, Sep. Purif. Technol., 92 (2012) 106–114.

[53] X. Guan, J. Ma, H. Dong, L. Jiang, Removal of arsenic from water: effect of calcium ions on As(III) removal in the $KMnO_4$–Fe(II) process, Water Res., 43 (2009) 5119–5128.

[54] J.C. Hsu, C.J. Lin, C.H. Liao, S.T. Chen, Evaluation of the multiple-ion competition in the adsorption of As(V) onto reclaimed iron-oxide coated sands by fractional factorial design, Chemosphere, 72 (2008) 1049–1055.

[55] V. Tanboonchuy, N. Grisdanurak, C.H. Liao, Background species effect on aqueous arsenic removal by nano zero-valent iron using fractional factorial design, J. Hazard. Mater., 205–206 (2012) 40–46.

[56] M.S.H. Mak, P. Rao, I.M.C. Lo, Effects of hardness and alkalinity on the removal of arsenic (V) from humic acid-deficient and humic acid-rich groundwater by zero-valent iron, Water Res., 43 (2009) 4296–4304.

[57] L. Wang, D.E. Giammar, Effects of pH, dissolved oxygen, and aqueous ferrous iron on the adsorption of arsenic to lepidocrocite, J. Colloid Interface Sci., 448 (2015) 331–338.

[58] D.J. Ridder, T.S.C.M. Wetering, T. Dijk, D. Halem, Influence of HPO_4^{2-}, H_4SiO_4, Ca^{2+}, Mg^{2+} on Fe floc growth and As(III) removal in aerated, natural groundwater, J. Water Process Eng., 25 (2018) 149–156.

[59] P. Mondal, A.T.K. Tran, B. van der Bruggen, Removal of As(V) from simulated groundwater using forward osmosis: effect of competing and coexisting solutes, Desalination, 348 (2014) 33–38.